PULL-IN TIME DYNAMICS AS A MEASURE OF ABSOLUTE PRESSURE

Raj K. Gupta and Stephen D. Senturia

Microsystems Technologies Laboratories, Rm. 39-567

Massachusetts Institute of Technology, Cambridge, MA 02139 USA

January 1997

PULL-IN TIME DYNAMICS AS A MEASURE OF ABSOLUTE PRESSURE

Raj K. Gupta and Stephen D. Senturia
Microsystems Technologies Laboratories, Rm. 39-567
Massachusetts Institute of Technology, Cambridge, MA 02139 USA

ABSTRACT

The squeezed-film damping component of the pull-in time of an electrostatically-actuated micromechanical fixed-fixed beam is shown to be a sensitive, and nearly linear function of ambient air pressure in the measured range of 0.1 mbar to 1013 mbar (1 atm or 760 Torr). Pull-in time simulations, based on a one-dimensional macromodel using a damping constant proportional to pressure, are in good agreement with measured data. The data and simulations show that pull-in type devices will make excellent microelectromechanical systems (MEMS) sensors for broad-range absolute pressure measurements and for *in situ* leak monitoring of hermetically sealed packages containing other sensors or IC's. The pull-in sensors are compatible with any MEMS fabrication processes that allow out-of-plane electrostatic actuation, including surface micromachining and silicon wafer-bonding, and they do not require a cavity sealed at vacuum or at a reference air pressure.

INTRODUCTION

A deformable parallel-plate structure electrostatically actuated across a narrowing gap becomes unstable beyond its static pull-in voltage (V_{PI}), a point at which the structure collapses, and makes contact to the opposing electrode, either directly, or on top of a standoff dielectric [1]. Pull-in type devices operated in a mechanically static contact/non-contact mode, are found in microrelays, deformable mirror devices (DMD's), grating light valves (GLV's), and mechanical property test structures [2-6].

When a pull-in structure is dynamically actuated by an applied step voltage V_{APP} greater than V_{PI}, the pull-in time (t_{PI}) is measured as the delay between the step bias application and the structure's contact to the bottom electrode. Simulations of the large amplitude dynamics of this coupled elastomechanical-electrostatic-compressible squeezed-film damping (CSQFD) system have shown general agreement to measured pull-in times versus V_{APP} in one atmosphere and in vacuum [7,8]. Modelling of the CSQFD is based on the compressible isothermal Reynold's equation for nonslip-flow models in [7,9], and for slip-flow models of dynamic rigid plates in [10]. Empirical reduced-order macromodels have also been applied to vertically damped structures with reasonable success in [7,11,12a], and are useful because of their simplicity.

The experiments in [7] show more than an order of magnitude difference between the pull-in times in air and in vacuum. This paper reports the measurement and simulation of a fixed-fixed beam's pull-in time as a function of arbitrary pressure, and exploits t_{PI}'s sensitivity to pressure for use as a sensor.

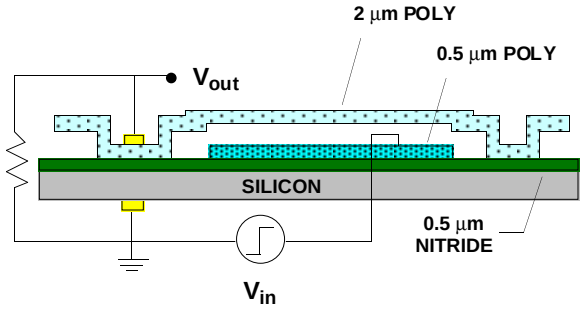

Figure 1: Circuit used for measuring pull-in times.

EXPERIMENTAL RESULTS

The surface-micromachined polysilicon fixed-fixed beam investigated in this study has a length (L) of 610 μm, a thickness (t) of 2.2 μm, a width (w) of 40 μm, and an undeflected gap (g) of 2.3 μm [13]. Using the circuit in Figure 1, the beam is electrostatically actuated by a 10 V (V_{APP}) zero-to-step bias, which is greater than its static pull-in voltage of 8.76 V. The t_{PI} is determined from switch closure, as shown in Figure 2.

Pull-in times for this beam are measured as a function of ambient air pressure. Figure 3 shows that t_{PI} asymptotically approaches a vacuum limit (t_{PI0}) of 18.2 μs, which is determined by the inertia of the system. When t_{PI0} is

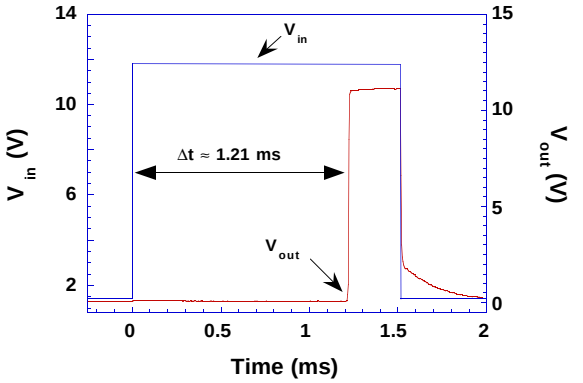

Figure 2: Oscilloscope data from a beam showing the procedure for measuring Δt, the pull-in time from its static deflection near 1.3 V to pull-in after application of 11.8 V. Note, the V_{in} and V_{out} axes are offset and scaled for clarity.

0-7803-3744-1/97/$5.00 © 1997 IEEE.

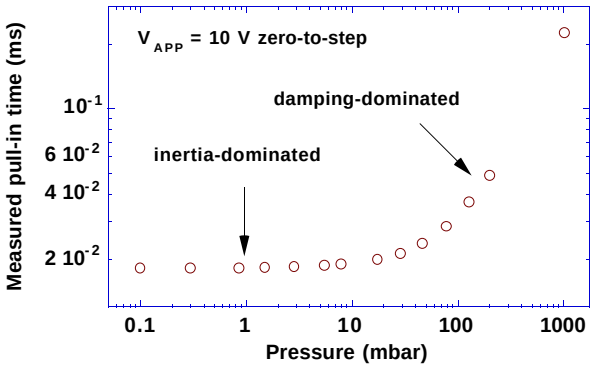

Figure 3: Pull-in times as a function of ambient air pressure of a 10 V zero-to-step actuated 610 μm long fixed-fixed beam, nominally 2 μm thick, 40 μm wide and with a 2 μm nominal gap. The low pressure asymptote is at t_{PI0} = 18.2 μs.

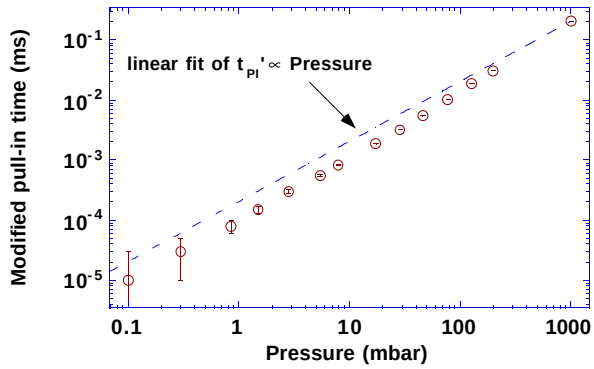

Figure 4: The modified pull-in time $t_{PI}' = (t_{PI} - t_{PI0})$, shown as circles, is obtained from the measured data in Figure 3. It is plotted versus ambient air pressure alongside a linear fit (dashed line). The 1D macromodel, using an empirically determined damping constant proportional to pressure, agrees almost identically with the dashed line fit.

subtracted from t_{PI}, the resulting modified pull-in time t_{PI}', varies almost linearly with pressure over four-orders of magnitude in pressure, as shown in Figure 4.

MACROMODEL SIMULATION

CSQFD simulations used in [7] indicate that for V_{APP} between V_{PI} and 5/4 V_{PI}, the velocity is constant for more than 3/4 of t_{PI}. Furthermore, in this region, the beam moves through only a small fraction of the total gap. Hence, the electrostatic force does not change significantly for most of the transient, and the damping force is relatively constant. This scenario is similar to an object moving through a viscous medium at terminal velocity obeying Stokes' law, where the damping force is proportional to velocity [14]. Based on this analogy, we conclude that a correct first-order damping term for the nonlinear pull-in dynamics will be well represented by a standard linear damping force proportional to velocity.

In the limit of linear damping, a one-dimensional (1D) lumped mass-spring-damper macromodel is helpful in understanding the experimental results in Figures 3 and 4 [7,11,12a]. The 1D macromodel is also useful in understanding ways to control the pressure sensitivity of a sensor. This will be discussed in a later section of our paper.

As shown in Figure 5, the mass of the 1D macromodel moves along the *x*-coordinate, and the electrostatic force is derived from the voltage across the parallel plate capacitance of area *A* with a gap *(g-x)*. The equation of motion for the 1D system is given by (1).

$$\underset{\text{inertia term}}{m\ddot{x}} + \underset{\text{damping term}}{b\dot{x}} + \underset{\text{spring term}}{kx} = \underset{\text{electrostatic term}}{\frac{\varepsilon_o A V_{APP}^2}{2(g-x)^2}} \qquad (1)$$

The spring constant (k), equal to 4.60 N/m, is determined by matching the 1D equation for $V_{PI} = (8kg^3/27\varepsilon_o A)^{1/2}$ to the statically measured V_{PI}, where $A = L \times w$. The mass (m), equal to 125 ng, is a product of L, w, t, and the polysilicon density $\rho = 2330$ kg/m^3. The damping constant (b) in the 1D model is determined by matching the experimental pull-in time at 1 atm to the corresponding pull-in time obtained from the numerical integration of equation (1). This yields a $b = 0.233$ g/s at 1 atm, which is then varied proportional to pressure to model t_{PI} data at arbitrary pressures. (Note, a similar approach, linearly varying viscosity for low pressures, was used in [12a].) Numerical integration of (1) based on the linear dependence b with pressure, calculates a t_{PI}' versus pressure relation which is indistinguishable from the linear fit in Figure 4.

At low pressures, the damping term in (1) can be neglected, and the system is inertia-dominated. This decreases the pull-in voltage for zero-to-step bias inputs

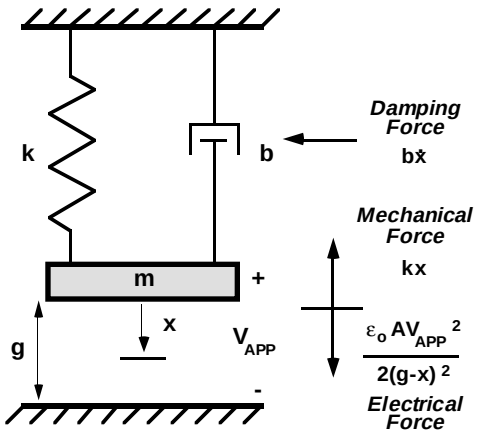

Figure 5: A schematic of the 1D macromodel.

to a new value V_{DPI}, which equals $(kg^3/4\varepsilon_o A)^{1/2}$. This result has been confirmed experimentally [7,8]. Furthermore, an analytic solution (2) can be obtained for t_{PI0}, where T_α equals $(m/k)^{1/2}$, and α equals V_{APP}/V_{DPI}. With the parameters given above, t_{PI0} is calculated to be 16.8 μs, which is close to the measured value of 18.2 μs.

$$t_{PI0} = \int_0^1 T_\alpha \left[\frac{\alpha^2}{4(1-y)} - \frac{\alpha^2}{4} - y^2 \right]^{-1/2} dy \quad (2)$$

At higher pressures, the 1D system will be damping-dominated, and the spring force will be negligible compared to the damping force. In this limit, t_{PI} will be given by equation (3), where T_β equals (b/k), and β equals V_{APP}/V_{PI}.

$$t_{PI} = T_\beta \int_0^1 \frac{27(1-y)^2}{4\beta^2 - 27\, y(1-y)^2} dy \quad (3)$$

At 1 atm, equation (3) calculates a t_{PI} equal to 233 μs, which is close to the measured value of 235 μs. Note, if the assumption of linear damping is still valid for $V_{APP} \gg V_{PI}$, the inertial term can also be neglected from (1), and t_{PI} will become independent of the structure's mechanical properties, as shown in equation (4).

$$t_{PI} \approx \frac{2bg^3}{3\varepsilon_o A V_{APP}^2} \quad (4)$$

A PRESSURE SENSOR DESIGN EXAMPLE

The assumption of a low Reynold's number regime ($R < 1$) in the CSQFD models of [7, 9, 10, 15] is valid in continuum flow for small device geometries and velocities. Reasoning back to our previous Stokes' law creeping flow analogy for incompressible fluids in this regime, we can represent the damping force (F_D) of a normally moving, thin circular plate, of diameter D, as,

$$F_D = C_D' \eta D V \quad (5)$$

where, C_D' is the viscous drag coefficient, which is dependent on the plate shape, η is the air viscosity, and V is the plate velocity [14]. For a circular shape C_D' equals 8. The linear damping force dependence on a plate's lateral dimension can be used to adjust the damping coefficient of a pull-in pressure sensor, and hence, its pull-in time sensitivity.

A conceptual design of a sensor with a thin uniform thickness is shown in Figure 6. Analogous to the equation (5) damping dependence on D of the circular plate, the damping dependence of a square plate will be linearly related to its width (w_s). Note that V_{PI} will be independent of w_s since the electrostatic load, which is determined by the width (w_c) of the underlying square contact, will be mainly carried by the mechanical deformation of the narrow cantilever supports.

Using equation (3) from the 1D model, the linear increase in b with w_s predicts that in the damping-dominated regime, t_{PI} will scale proportionally with w_s. Similarly, in the inertia-dominated limit, equation (2) predicts that t_{PI0} will scale with $m^{1/2}$, which is linearly dependent on w_s. These results indicate that an increase in w_s will produce a vertical shift in the t_{PI} versus pressure relation.

Rough calculations using the 1D model, where b is proportional to pressure, indicate that the pressure of transition (P_t) from the inertia-dominated regime to the damping-dominated regime will occur when $b/(mk)^{1/2} \sim 1$. Based on the 1D model of the data presented in Figure 3, this relation correctly estimates that $P_t \approx 100$ mbar.

The above relation can also be used to tailor P_t, such that lowering it will reduce the subtraction error in t_{PI}' at low pressures. For the square plate, $b/m^{1/2}$ is independent of w_s. However, by reducing the tensile stress in the beams, k, which is independent of $b/m^{1/2}$, decreases and, therefore, decreases P_t. Similarly for k of a thin beam, P_t varies inversely with t^2 in pure bending, and with t in pure tension.

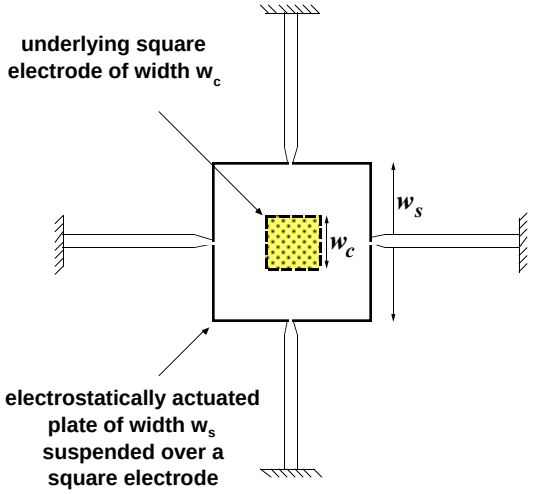

Figure 6: A conceptual design for a pull-in pressure sensor that can be tailored to a specific pressure range. The area of the square electrode of width w_c controls the electrostatic force which appears as a tip load on the four supporting cantilevers of the relatively rigid square plate of width w_s. The cantilever's length and width, and the square electrode's area determine V_{PI}. The movable plate area determines the air damping, and can be varied to adjust the pressure sensitivity of the sensor.

DISCUSSION

The pull-in sensor measures absolute pressure, unlike overpressure-limited or touch-down-mode sealed-cavity differential pressure sensors. Some differential sensors measure pressure-induced deflections in diaphragms by small changes in capacitance or in tunneling current [16-19]. Other differential pressure sensors measure diaphragm deflection by using resonant strain-gauges on top of the diaphragms, and are encapsulated at low pressures needed for high quality factors (Q) [20,21].

Other absolute pressure sensors, which utilize a shift in mechanical resonant frequency from high squeeze-numbers in CSQFD, require large flat area devices $(1.2\ \text{mm})^2$ with small gaps ($\sim 1\ \mu\text{m}$) and no etch/release holes [12b]. They have a high pressure limit as Q approaches one [9]. Another type of an absolute sensor is based on measuring thermal conduction to the surrounding gas [22,23]. These appear to have poor resolution at low pressures where conductive heat transfer may be on the order of radiative cooling.

The pull-in sensor is advantageous in that it can be easily microfabricated alongside other micromachined sensors, and that it can serve as an *in situ* monitor for pressure with these sensors or IC's. This is important, for example, in measuring leaks in a hermetically sealed micromachined accelerometer package that must maintain critical damping in a narrow range of pressure [15].

Experience to date suggests that stiction of the pull-in sensors can be avoided if a low enough operating voltage is chosen. An experiment, using a low frequency (< 10 Hz) square-wave excitation on a beam of the type investigated here, was conducted in air at 1 atm over more than a million continuous cycles without showing an observable drift in t_{PI}.

Sutherland's expression for the temperature (T) dependence of η, as shown in (6), indicates from (5) that the damping force of the pull-in sensor will be sensitive to temperature [24]. In equation (6), C is a measure of the attractive molecular forces, and is ~ 100 K for air at 1 atm. η_0 is the dynamic viscosity measured at the reference temperature T_0.

$$\frac{\eta}{\eta_0} = \left(\frac{T}{T_0}\right)^{\frac{1}{2}}\left(\frac{1 + C/T_0}{1 + C/T}\right) \qquad (6)$$

While this is not a strong temperature dependence, an *in situ* temperature sensor may be needed to compensate for temperature variations.

CONCLUSIONS

The application of a pull-in device to a MEMS pressure sensor is clear. It is simple to design and easy to test. When a simple beam's modified pull-in time is plotted versus four-orders of magnitude in pressure, it scales proportionately. The pull-in/response time for the beam was a few milliseconds or less, and could be simulated with an empirical 1D macromodel. Also predicted by the 1D model for damping in low Reynold's number regimes was that the pull-in time can be scaled for pressure sensitivity by adjusting a critical lateral dimension of a pull-in device. The pull-in time for the beam at 1 atm was found to be stable over a million cycles, and under appropriate biasing conditions, the device was repeatably operated without stiction.

ACKNOWLEDGMENTS

This work was sponsored in part by the Semiconductor Research Corporation (Contract 95-SC-309) and by ARPA (Contracts J-FBI-92-196 and J-FBI-95-215).

REFERENCES

[1] H. C. Nathanson, W. E. Newell, R. A. Wickstrom, and J. R. Davis, Jr., "The Resonant Gate Transistor", *IEEE Transactions on Electron Devices*, **ED-14**, No. 3, March 1967, pp. 117-133.

[2] M.-A. Gretillat, P. Thiebaud, N. F. de Rooij, and C. Linder, "Electrostatic Polysilicon Microrelays Integrated with MOSFETs", *Proceedings of MEMS 1994*, Oiso, JAPAN, January 1994, pp. 97-101.

[3] L. J. Hornbeck, "128 × 128 Deformable Mirror Device", *IEEE Transactions on Electron Devices*, **ED-30**, (1983), p. 539.

[4] R. B. Apte, F. S. A. Sandejas, W. C. Banyai, and D. M. Bloom, "Deformable Grating Light Valves for High Resolution Displays", *Proceedings of the 1994 Solid-State Sensor and Actuator Workshop (Invited Paper)*, Hilton Head, SC, June 13-16, 1994, pp. 1-6.

[5] K. Najafi and K. Suzuki, "A Novel Technique and Structure for the Measurement of Intrinsic Stress and Young's Modulus of Thin Films", *Proceedings of MEMS 1989*, Salt Lake City, February 1989, pp. 96-97; K. Najafi and K. Suzuki, "Measurement of Fracture Stress, Young's Modulus, and Intrinsic Stress of Heavily Boron-Doped Silicon Microstructures", *Thin Solid Films*, **181** (1989), pp. 251-258.

[6] R. K. Gupta, P. M. Osterberg, S. D. Senturia, "Material Property Measurements of Micromechanical Polysilicon Beams", *Proceedings of SPIE 1996 Conference (Invited Paper): Microlithography and Metrology in Micromachining II*, Austin, TX, October 14-15, 1996, pp. 39-45.

[7] R. K. Gupta, E. S. Hung, Y.-J. Yang, G. K. Ananthasuresh, and S. D. Senturia, "Pull-in Dynamics of Electrostatically-Actuated Beams", *Proceedings of the 1996 Solid-State Sensor and Actuator Workshop, Late News Session*, Hilton Head, SC, June 3-6, 1996, pp. 1-2; R. K. Gupta, E. S. Hung, Y.-J. Yang, G. K. Ananthasuresh, and S. D. Senturia, "Pull-in Dynamics of Electrostatically-Actuated Microstructures", *Semiconductor Research Corporation (SRC) TECHCON 1996*, Phoenix, AZ, September 1996.

[8] G. K. Ananthasuresh, R. K. Gupta, and S. D. Senturia, "An Approach to Macromodeling of MEMS for Nonlinear Dynamic Simulation", *ASME 1996 International Mechanical Engineering Congress and Exposition, Symposium on MEMS, Proceedings of Dynamics Systems and Controls*, DSC-Volume 59, Atlanta, GA, November 17-22, 1996, pp. 401-407.

[9] Y.-J. Yang and S. D. Senturia, "Numerical Simulation of Compressible Squeezed-Film Damping", *Proceedings of the 1996 Solid-State Sensor and Actuator Workshop*, Hilton Head, SC, June 3-6, 1996, pp. 76-79.

[10] C.-L. Chen and J. J. Yao, "Damping Control of MEMS Devices Using Structural Design Approach", *Proceedings of the 1996 Solid-State Sensor and Actuator Workshop*, Hilton Head, SC, June 1996, pp. 72-75.

[11] T. Veijola, H. Kuisma, J. Lahdenperä, and T. Ryhänen, "Equivalent-Circuit Model of the Squeezed Gas Film in a Silicon Accelerometer", *Sensors and Actuators A*, **48** (1995), pp. 239-248.

[12] (a) M. Andrews, I. Harris, and G. Turner, "A Comparison of Squeeze-film Theory with Measurements on a Microstructure", *Sensors and Actuators A*, **36** (1993), pp. 79-87; (b) M. Andrews, G. Turner, P. Harris, and I. Harris, "A Wide Range Pressure Sensor Using the Squeeze Film Effect", *Proceedings of Transducers' 93*, Yokohama, JAPAN, June 7-10, 1993, pp. 214-216.

[13] MUMPs 5 devices courtesy of Karen Markus and David Koester of MCNC.

[14] P. M. Gerhart and R. J. Gross, "Fundamentals of Fluid Mechanics", Addison-Wesley, 1985, pp. 509-538.

[15] R. P. van Kampen, M. J. Vellekoop, P. M. Sarro, and R. F. Wolffenbuttel, "Application of Electrostatic Feedback to Critical Damping on an Integrated Silicon Capacitive Accelerometer", *Sensors and Actuators A*, **43** (1994), pp. 100-106.

[16] L. Parameswaran, A. Mizra, W. K. Chan, and M. A. Schmidt, "Silicon Pressure Sensors Using a Wafer-bonded Sealed Cavity Process", *Proceedings of Transducers' 95 • Eurosensors IX, Volume 2*, Stockholm, SWEDEN, June 25-29, 1995, pp. 582-585.

[17] Y. Zhang and K. D. Wise, "A High Accuracy Multi-Element Silicon Barometric Pressure Sensor", *Proceedings of Transducers' 95 • Eurosensors IX, Volume 1*, Stockholm, SWEDEN, June 25-29, 1995, pp. 608-611.

[18] W. H. Ko, Q. Wang, and Y. Wang, "Touch Mode Capacitive Pressure Sensors for Industrial Applications", *Proceedings of the 1996 Solid-State Sensor and Actuator Workshop*, Hilton Head, SC, June 3-6, 1996, pp. 244-248.

[19] C. Yeh and K. Najafi, "Bulk-Silicon Tunneling-Based Pressure Sensors", ***Proceedings of the 1994 Solid-State Sensor and Actuator Workshop***, Hilton Head, SC, June 13-16, 1994, pp. 201-208.

[20] D. W. Burns, J. D. Zook, R. D. Horning, W. R. Herb, and H. Guckel, "A Digital Pressure Sensor Based on Resonant Microbeams", *Proceedings of the 1994 Solid-State Sensor and Actuator Workshop*, June 13-16, 1994, pp. 221-224.

[21] C. J. Welham, J. W. Gardner, and J. Greenwood, "A Laterally Driven Micromachined Resonant Pressure Sensor", *Proceedings of Transducers' 95 • Eurosensors IX, Volume 2*, Stockholm, SWEDEN, June 25-29, 1995, pp. 586-589.

[22] S. D. James, R. G. Johnson, and R. E. Higashi, "A Broad Range Absolute Pressure Sensor", *Proceedings of 1988 IEEE Solid-State Sensor and Actuator Workshop*, Hilton Head, SC, June 6-9, 1988, pp. 107-108.

[23] C. H. Mastrangelo and R. S. Muller, "Fabrication and Performance of a Fully Integrated μ-Pirani Gauge with Digital Readout", *Proceedings of Transducers' 91*, San Francisco, CA, June 24-27, 1991, pp. 245-248.

[24] S. Dushman, "Scientific Foundations of the Vacuum Technique, Second Edition", John Wiley & Sons, Inc., 1962, pp. 28-33.